RSC Advances

ROYAL SOCIETY OF CHEMISTRY

www.rsc.org/advances

Cite this: DOI: 10.1039/c0xx00000x

www.rsc.org/xxxxxx

ARTICLE TYPE

Dye adsorbed on copolymer, possible specific sorbent for metal ions removal

Simona Gabriela Muntean,*[a] Maria Elena Rădulescu-Grad[a], and Paula Sfârloagă[b]

Received (in XXX, XXX) Xth XXXXXXXXX 20XX, Accepted Xth XXXXXXXXX 20XX

DOI: 10.1039/b000000x

The efficiency of styrene-divinylbenzene functionalized with trimethylamonium groups as sorbent for the direct dye removal from aqueous solutions was investigated. The influence of process variables such as initial concentration, temperature and pH was developed. The amount of adsorbed dye - was favorized at higher initial dye concentrations, while the removal percentage decreased. The increase of the temperature induced a positive effect on the adsorption indicating that the process is endothermic. The maximum removal percentage was obtained in acidic medium. The adsorption kinetics followed the pseudo-second-order equation, with regards to the intra-particle diffusion rate. The experimental data was well correlated by the Sips adsorption model, and the maximum theoretical adsorption capacity was determined to be 83.75 mg dye/g copolymer. The new obtained specific sorbent (dye-attached to copolymer) was investigated in removal of heavy metals ions (Cu, Zn). Very high adsorption rates were observed at the beginning of the adsorption process and the equilibrium was achieved in about 5 minutes.

Introduction

Industries such as textile, paper, plastics, etc., use huge volumes of water and chemical substances for colouring the manufactured articles, and discharge large amounts of wastewater during industrial processing. Effluents discharged are aesthetically unpleasant, and can produce serious pollution problems [1, 2]. The presence of the synthetic dyes in nature, non biodegradable, and toxic to some organisms, has a noxious effect on the environment (water and soil).

Direct dyes are water-soluble dyes widely used in the Romanian textile dyeing industry. They tend to pass through conventional treatment unaffected so their removal from wastewater is highly difficult. In living organisms, some of these dyes can produce carcinogenic, and mutagenic aromatic amines in the reductive degradation process, under the action of the enzyme, and intestine microflora [3, 4]. International organizations such us IARC (International Agency for Research on Cancer), and ETAD (Ecological and Toxicological Association of the Dyestuffs Manufacturing) developed several compounds containing aromatic amines with carcinogenic, mutagenic, and teratogenic characteristics [5, 6]. Synthesis of benzidinic direct dyes was forbidden, due to the carcinogenic activity of benzidine and most of its derivatives [7]. Finding substitutes for this kind of compounds represents an increased demand and a relevant subject, and discharge of dye pollutants became an ecological concern.

Several methods (coagulation/flocculation [8, 9], chemical oxidation [10], membrane separation [11], adsorption [12-14], electrochemical reduction [15], microbiological decomposition [16], extraction [17] etc.) have been developed to remove color from dye-containing effluent, varying in effectiveness, economic cost and environmental impact. The adsorption process provides an attractive alternative method for the treatment of dye-contaminated waters because of its simplicity, selectivity and efficiency [18-20]. In the recent years, there is a growing interest for the adsorption capacities of synthetic polymeric adsorbents. Due to their diversity in surface and porosity, high physical-chemistry stability, polymeric adsorbents have been used as alternative to activate carbon in removal and recovery of organic pollutants from industrial wastewaters [21-23]. The dye adsorption process is mainly dependent on the dyes' structure, and the surface chemistry of the adsorbents, chemical modification being an effective approach for improving adsorption performance of a polymeric adsorbent toward dye removal [24].

The presence of heavy metal ions in the environment is one of the major concerns due to their toxicity to many life forms [25]. Treatment of waste waters containing heavy-metal ions requires concentration of the metals into a smaller volume followed by recovery or secure disposal. Heavy–metal ions can be removed by adsorption on solid carriers using either non-specific or specific sorbents [26-28]. Specific sorbents consist of a carrier matrix, and a ligand (*e.g.*, ion-exchange material or chelating agents) which interacts with the metal ions specifically.

The aim of the present work was to investigate the efficiency of a synthetic copolymer, in the direct dye removal from aqueous solutions. In order to this equilibrium and kinetic studies have been carried out. The influences of process variables such as time, initial concentration, temperature and pH have been investigated.

Experimental

Materials

The trisazo direct dye (*AHDS*) derived from 4,4'-diamino-benzanilide has been synthesized in order to obtain very good substitutes of its homologue benzidinic dye C.I. Direct Brown as described in a previous paper [29].

The pH values of the solutions were adjusted by using HCl or NaOH (0.02 M), and were measured using a WTW model 330i pH meter.

The p(StDVB-NMe) was prepared by the polymer-analogous reaction as previously described [30]; StDVB-ClMe was aminated by adding 25 ml of 25% trimethylamine in ethanol and stirring at room temperature for 24 hours. An excess of trimethylamine was used in comparison to the chloromethyl content of the copolymer. The resulting product was washed afterwards with methanol, water, and acetone, dried at 50°C in a vacuum oven until reached a constant weight, and characterized by UV-VIS and FTIR spectroscopy.

Physico-chemical determinations

The morphological characterization of the copolymer microbeads, before and after dye attaching, was performed by scanning electron microscope (INSPECT-S), at 10 nm, 3 kV in high-vacuum modul.

The nitrogen content from the p(StDVB-NMe) and dye-attached to microbeads has been performed by Energy Dispersive X-ray (EDX) analysis on the Quanta 200 (FEI) electron microscope equipped with EDX system.

FT-IR spectroscopy Fourier Transform Infrared Spectroscopy (FT-IR) spectra were obtained from a JASCOFT/IR 4200 spectrometer (JASCO Corp., Japan) on 400–4000 cm^{-1} range at $4cm^{-1}$ spectral resolution. Solid samples were prepared as KBr pellets.

The dye concentration in solution at initial time and at time *t* was spectrophotometrically measured using a CECIL CE 7200 Spectrophotometer in the wavelength range 250 to 750 nm.

The metal ions concentrations in the aqueous phases were measured by using an Atomic Absorption Spectrophotometer PYE UNICAM SP1900.

Methods

The dye adsorption on the copolymer microbeads have been studied in aqueous solutions in a batch system. For the dye immobilization 100 mL dye solution and 0,1g copolymer were magnetically stirred at 250 rpm for a specific time *t*. After reaching the equilibrium, the colored microspheres were separated through filtration, washed with distilled water (2×20 mL), and dried at 30°C for 24 hour.

The effect of initial concentration, temperature and solution pH on the dye adsorption was investigated.

Using the obtained experimental values the adsorption capacity (Eq. 1) and the removal percentage (η) have been calculated (Eq. 2):

$$q_t = \frac{(C_0 - C_t)\cdot V}{W} \quad (1)$$

where: q_t is the amount of dye adsorbed onto the copolymer unit at time *t* (mg/g), C_0 and C_t are the dye concentration in solution at initial time, and at time *t* (mg/L), *V* is the solution volume (L), and *W* is the amount of adsorbent (g);

$$\eta = \frac{C_0 - C_e}{C_0}\cdot 100 \quad (2)$$

where: C_e is dye concentration at equilibrium (mg/L).

Aqueous solution (20 mL) containing different amounts of copper and zinc ions (5-100 ppm) and 0.2 g specific sorbent (*AHDS* dye-attached to p(StDVB-NMe)) were stirred at 500 rpm, at room temperature in the Berzelius flasks, in the pH range 2-7, adjusted with universal buffer solution. After three hours the metal-colored microbeads were separated by filtration.

Results and discussion

The chemical structure and the characteristics of the *AHDS* dye are presented in Figure 1, and Table 1. It reveals the presence in the dye molecule of characteristic functional groups (OH, NH2, COOH) located at various positions in the molecule with the ability to form complexes (chelates) with ions of transition metals.

Figure 1.

Table 1.

Schematic representation of the copolymer structure is presented in Figure 2. The presence of the quaternary ammonium groups is shown.

Figure 2.

AHDS was attached to the microbeads via electrostatic interaction between the sulphonic group of its and the chloride of the StDVB-ClMe, by ion-exchange mechanism, according to the Figure 3.

Figure 3.

The amount of dye attached on the microbeads was evaluated by using an elemental analysis instrument by considering the nitrogen and sulphur stoichiometry (Tabel 2).

Characterization of copolymer microbeads

The dye adsorption process was followed by washing with distilled water and the copolymer remained uniform colored.

The copolymeric adsorbent, before and after adsorption experiments, was characterized by electron micrographs in order to evaluate the sorbent's surface morphology. The microbeads present a uniform and spherical form with almost compact structure, and smooth surface characteristics (Figure 4).

Figure 4.

An increase of the pore size average from 236.7 μm to 256.98 μm has been observed after the dye adsorption probably due to the swelling of the microbeads by dye adsorption

The elemental analysis of the unmodified p(StDVB-NMe) and dye-attached beads were carried out, and the attachment of the dye was confirmed by an increase of the nitrogen level from 4.93 to 7.09, and the presence of the sulphur in the dye-attached beads (Table 2).

Table 2.

The infrared spectroscopy was used to monitor the functional group presence/changes during the adsorption process. A detailed FT-IR characterization of the free and attached *AHDS* dye onto anion exchanger p(StDVB-NMe) was carried out (Supp Figure 1). The FT-IR spectra of the StDVB-MeN microbeads present characteristic absorption bands at 3020 cm^{-1}, 827 cm^{-1}, and 891 cm^{-1} corresponding to C-H (sp^2) of aromatic ring; at 1549.2 cm^{-1}, 1514.81 cm^{-1}, and 1644.02 cm^{-1} bands characterisc for the C=C phenyl stretching; bands at 751.2 cm^{-1} and 696.2 cm^{-1} attributed to the presence of out of plane bending of monosubstituted benzenes, and a broad peak in the area of 3100 – 3600 cm^{-1} corresponding to the $–CH_2N^+Me_3$ moiety. The evidence of resin amination corresponding to tertiary amine stretching is revealed by the presence of bands at 2354.66 cm^{-1} [31].

The *AHDS* direct dye spectra present an intense band assigned to phenolic hydroxyl (3455.81 cm^{-1}), specifically vibration of aromatic ring (760.78 cm^{-1}, 838.88 cm^{-1}, 1323.89 cm^{-1}), conjugated aromatic ring (1483.96 cm^{-1}), sulphonic group (1044.26 cm^{-1}, 1172.51 cm^{-1}), carboxyl and amidic stretching (1226.5 cm^{-1}, 1279.54 cm^{-1}, 1599.66 cm^{-1}, 1662.34 cm^{-1},) phenolic hydroxyl (637.36 cm^{-1}, 1018.23 cm^{-1}, 1139.720 cm^{-1}), and nitro group (838.88 cm^{-1}, 1599.66 cm^{-1}).

In the AHDS-p(StDVB-NMe) polymer FT-IR spectra besides the polymer characteristic bands a band at 1483.95 cm^{-1} corresponding to the N=N vibration absorption and the characteristic bands of functional groups -SO_3 1034.62 cm^{-1}, 1093.44 cm^{-1}, and 1093.44 cm^{-1} could be observed, which indicate the presence of the dye onto the polymer microbeads surface. The amide group from the dyes, lead to the changes in the 3100 – 3500 cm^{-1} region due to the N-H stretch vibration.

We can assume that the *AHDS* dye sorption mechanism onto the p(StDVB-NMe) may be attributed to the chemical reaction between the protonated quaternary ammonium groups (-$N^+(CH_3)_3Cl^-$) of the anion exchanger and the dye anions (R-SO_3^- Na^+).

Effect of initial dye concentration and contact time

The effect of the initial dye concentration depends on the relation between the active centre available on an adsorbent surface and the dye concentration. The effect of the dye concentration and contact time have been investigated at pH 7, 318K in three concentration levels in the range of 10^{-5} -10^{-4} mol/L. The results, depicted in Figure 5a indicate that the adsorption is rapid in the initial stages and after reaching the equilibrium time, it remains nearly constant due to the saturation of the active centre available for dye on the adsorbent surface [32, 33]. The necessary time for reaching the equilibrium increased with the increasing of the dye concentration due to the fact that adsorption occurred both at the surface, and in the pores of the polymer, and the diffusion into the internal adsorption sites is stimulated by the increasing of the initial dye concentration. The amount of adsorbed dye increased from 8.85 to 81.48 mg/g while the percentage removal decreased from 98.44 to 90.63, with the increase in the initial dye concentration (Table 3) from 8.99 to 89.9 mg/g, indicated that the dye removal is concentration dependent.

Figure 5.

Table 3.

For lower concentrations, the ratio of number of dye molecules to the available adsorption sites is low, and increase with increasing the concentration. The increase in the initial dye concentration will cause an increase in the loading capacity of the adsorbent may be due to the high driving force for mass at a high initial dye concentration [34].

We obtained very good results (greater than 85%) in the dye removal percentage at low concentrations.

The results are in agreement with the data reported before (Table 4) and clearly demonstrated that p(StDVB-NMe) can be used as a novel alternative adsorbent for the purification of colored wastewaters.

Table 4

Effect of Temperature

The effect of temperature on the sorption process was studied at three different temperatures (i.e., 303, 318, 333 K) at pH 7, and 46.97 mg/L dye concentration. These ranges of temperatures have been chosen in order to obtain results as closely as possible with normal working conditions, and with minimum working costs. A comparison of experimental data (Figure 5b, Table 3) shows that the rise of temperature induced a positive effect on the sorption capacity (removal percentage increased from 77.46% to 98.2%), and a decrease of the necessary time for reaching the equilibrium from 170 to 105 min, which is in accordance with studies of Al-Ghouti [40] and Hiroyuki [41]. The increase of dye removal with increasing temperature may be attributed to the increase of the dye mobility, the decrease of the thickness of the boundary layer surrounding the adsorbent, thus, decrease the mass transfer resistance of adsorbate [42].

Effect of pH

The dye solution pH value plays an important role in the whole adsorption process and particularly on the adsorption capacity [32, 43]. The degree of adsorption of the dye's ions onto the adsorbent surface is primarily influenced by the surface charge on the adsorbent, which in turn is influenced by the solution pH [44, 45]. *AHDS* dye is negatively charged in solution (-SO_3^-, -COO^-), having an affinity to materials with positive charges, which is the case of p(StDVB-NMe), with positively charged functional groups (-NMe_3^+).

The effect of pH has been evaluated in the range of 4 to 10 in by using 44.95 mg/g dye at 303 K in order to determine the optimum pH value at which the dye removal percentage is maximum. Thereafter the absorption analysis was done and the results are presented in Figure 5c.

With the increase of pH, a decrease in removal percentage from 84.87 to 57.73% was observed (Table 3). This may be due to electrostatic attraction between the negatively charged dye molecule, and the positively charged adsorption sites of the sorbent. The maximum removal percentage was found to be at pH 4.1. At low pH, the concentration of H^+ would be high, thus enhancing the high electrostatic attraction between the positively charged adsorbent surface and anionic dye *AHDS* [46]. The lower removal of the *AHDS* dye at higher pH is probably due to the OH^- ions excess competing with the anionic dyes for the adsorption sites of the sorbent.

Adsorption kinetics

In the kinetic experiment, the changes of absorbance were determined at certain time intervals during the adsorption process. The experimental results obtained for the influence of initial concentration were analyzed using first-order Lagergren model (Eq. 3), pseudo second-order model (Eq.4) and intraparticle diffusion model (5).

$$\log(q_e - q_t) = \log q_e - \frac{k_1}{2.303} t \quad (3)$$

$$\frac{t}{q_t} = \frac{1}{k_2 q_e^2} + \frac{1}{q_e} t \quad (4)$$

$$q_t = k_i t^{0.5} + l \quad (5)$$

where: k_1 is Lagergren rate constant (min^{-1}), k_2 is rate constant for the pseudo-second order adsorption model (g/mg min), k_i is the intraparticle diffusion rate constant (mg/g $min^{0.5}$) and l is the effect of boundary layer thickness.

The correlation coefficients were used to determine the best fitting kinetic model. The comparison of experimental adsorption capacities and the theoretical values, and the computed results estimated from equations 3, 4 and 5 are presented Table 5.

Table 5.

For the obtained data two model were tested in order to establish the best fitting equation. Very good coefficient R^2 values, compared to the first order obtained R^2 value, have been obtained when the pseudo-second order model have been evaluated, indicating that the chemical reaction is the main rate-controlling step of the adsorption process. These results are in concordance with the data reported by Dulman [32], Bayramoglu [39] and Tayyebeh [47]. Moreover, a decrease of the pseudo-second order rate constant k_2 was observed, indicating that the necessary time for reaching the equilibrium increased with increasing initial dye concentration.

The tinctorial process involves several steps: dye diffusion through solution to the outer surface of the adsorbent (film diffusion), dye adsorption on the outer surface of the adsorbent, dye diffusion from the surface into the adsorbent interior (internal diffusion) and, dye adsorption to the interior surface of the pores, as presented by Albergina and Fisichella [48]. In adsorption systems where there is the possibility of intraparticle diffusion being the rate-limiting step, the intraparticle diffusion approach described by Weber and Morris, 1963 is used (Eq. 5). All the plots (Figure 6) have same features, initial linear portion (the gradual adsorption stage) were intraparticle diffusion is rate-controlled, followed by a plateau (the final equilibrium stage) where intraparticle diffusion slows down.

Figure 6.

The plot did not pass through the origin, suggesting that adsorption involved intraparticle but was not the only rate-controlling step. From the plot of q_t versus $t^{0.5}$ the values of intraparticle diffusion rate constant (k_i), and the effect of boundary layer thickness (l) were calculated (Table 4). Maximum is the intercept length, adsorption is more boundary layer controlled.

Adsorption isotherms

For a better understanding or the adsorption process the equilibrium adsorption studies were carried out. Four adsorption models Freundlich, Langmuir, Sips, and Redlich-Peterson have been used to find the best isotherm for the experimental data obtained at equilibrium, at 318 K, and pH 7.2 (Table 6). The Freundlich adsorption model (Eq. 7) stipulates that the ratio of solute adsorbed to the solute concentration is a function of the solution. Langmuir developed a model (Eq. 8) based on the assumption that adsorption was a type of chemical combination or process and the adsorbed layer was unimolecular. Once a dye molecule occupies a site, no further sorption can take place at that site therefore, a saturation value is reached, beyond which no further sorption can take place. Sips improved the Freundlich and Langmuir equations with a new model (Eq. 9) which proposes that the equilibrium data follow the Freundlich model at low initial solute concentrations and the Langmuir one at high solute concentrations. The Redlich-Peterson isotherm (Eq. 10) unites the Langmuir and Freundlich isotherm, and its adsorption mechanism does not obey ideal monolayer adsorption, but an impure one [49, 50].

Table 6.

The experimental data have been analysed by using ORIGIN version 6.1. Software and the parameters which describe the theoretical models have been determined. Principal statistical criteria were the standard deviation (SE), the squared multiple regression coefficient (R^2), and the chi-square analysis (χ^2).

Chi-square test was use in order to confirm the best fit isotherm for the adsorption system combined with the values of the correlation coefficient.

The Chi square can be determined by equation (6):

$$\chi^2 = \sum \frac{(q_e - q_{e,m})^2}{q_{e,m}} \quad (6)$$

where: $q_{e\exp}$ is the equilibrium capacity (mg/g) obtained from experimental data, and $q_{e,m}$ is the equilibrium capacity obtained by calculating from the model (mg/g). A low value of χ^2 indicates that experimental data fit better to the value from the model

The comparisons between experimental data and fit sorption isotherm curves are presented in Figure 7, and the data obtained for the fitted models are presented in Table 7. The best isotherm model that fits the experimental data with lower error was the Sips isotherm model (Figure 7, Table 7). That means that adsorption process is going on after a combined model Frendlich and Langmuir: diffused adsorption on low dye concentration, and a monomolecular adsorption with a saturation value - at high adsorbate concentrations.

Figure 5.

Table 7.

The maximum adsorption capacity of the p(StDVB-NMe) have been determined to be 97.42 mg *AHDS* dye/g adsorbent. This result was obtained based on the sorption isotherm curves. The value higher or comparable with the data reported before (Table 4).

Metal ions removal

Because the studied dye has an o-hidroxycarboxilic and an o-amino-o'-carboxyazoic structure which allows formation of internal metallic complex, an extension of the study into the heavy metal ions removal was required.

In this preliminary research, the effect of the initial metal concentration on the adsorption rate and capacity was studied.

The quantity of adsorbed metal per unit mass of specific sorbent was assessed using the relation (1). Figure 8 shows the sorption of Cu(II) and Zn(II) by *AHDS* dye-attached to p(StDVB-NMe) as a function of contact time at different initial concentrations. The metal removal is rapid at the beginning of adsorption, and after approximately 15 minutes remains constant. The initial faster rate of metal removal may be explained by the large number of adsorption sites available for adsorption, and the plateau value represents the saturation of the copolymer active centres available for the metal ions.

Figure 8.

The amount of adsorbed metal ions per unit mass of copolymer (adsorption capacity) increased with the increase of the metal ions concentration, probably due to the rapid external mass transfer followed by a slower internal diffusion process. Besides the two tested metal ions adsorption capacity for Zn(II) ions (54.5 mg/g microspheres), was higher compared to the (2.8 mg/g microspheres) obtained for the Cu(II) ions, due to much higher affinity of immobilized dye molecules to the first species. The obtained results are in concordance with the results presented by Kicsi [53] and Yusoff [54].

It is well known that metal ion adsorption both on non-specific and specific sorbents is pH dependent. Therefore, in our preliminary study, the effect of pH on the adsorption of metal ions onto the *AHDS* dye-attached to p(StDVB-NMe) microspheres, have been evaluated in the range of 2-7. In these experiments, the initial concentration of metal ions was set at 30 ppm for Cu(II) and 100 ppm for Zn(II) ions. Figure 9 presents the specific adsorption of metal ions function on solution pH.

Figure 9.

The results depicted in Figure 7 indicate that, the heavy metal ions adsorption first increased with increasing pH and reached almost a constant value at pH~ 5. A high adsorption rate at alkaline pH values implies that metal ions interact with direct dye (AHDS) not only through the nitrogen atoms by chelating, but also through $-SO_3H$ groups by cation exchanges, which are unprotonated at high pH values.

These results indicate that the purposed polymer as sorbent have been successfully used for removal of heavy-metal ions from aqueous solutions, and encourage us to extend these researches.

Conclusions

The adsorption of direct dyes from colored solutions on a synthetic sorbent was carried out at different working conditions. By using infrared spectroscopy, and elemental analysis, we confirmed that direct dyes can be grafted by p(StDVB-NMe) copolymer. High removal percentage (greater that 85%) was obtained when low dye concentrations have been used, ambient temperature and neutral pH. Kinetic studies showed that the adsorption followed the pseudo-second-order reaction. The experimental data were well correlated by the Sips adsorption model, and the maximum theoretical adsorption capacities were determined. The rapid uptake and high sorption capacity make p(StDVB-NMe) a very attractive alternative sorbent material.

The preliminary study for the metal ions removal place the AHDS-p(StDVB-NMe) as a promising alternative adsorbent for the purification of wastewaters with minimal working costs.

Acknowledgement

This work was supported by Program 2 of Institute of Chemistry Timisoara of Romanian Academy (Research Project 2.3.).

Authors Information

[a] *Institute of Chemistry Timisoara of Romanian Academy, 24 Mihai Viteazul Str., 300223 Timisoara, Romania, tel: 0040256491818; fax: 0040256491824; E-mail: sgmuntean@acad-icht.tm.edu.ro;*
[b] *National Institute for Research and Development in Electrochemistry and Condensed Matter, Prof. dr. Aurel Paunescu Podeanu Str. 144, Timişoara, Romania;*

Notes

The authors declare no competing financial interest.

References

1. A.A. Ahmad, B.H. Hameed, N. Aziz, *J. Hazard. Mater*., 2007, **141**, 70.
2. U.G. de Aragao, H.S. Freeman, S.H. Warren, D. Palma de Oliveira, Y. Terao, T. Watanabe, L.D. Claxton, *Chemosphere*, 2005, **60**, 55.
3. A. Pielesz, I. Baranowska, A. Rybak, A. Wlochowicz, *Ecotox. Environ. Safe*. 2002, **53**, 42.
4. J. Wang, H.S. Freeman, L.D. Claxton, 2007, *Color. Technol*. **123**, 39.
5. Information Notice No. 6. German Ban of Use of Certain Azo Compounds in some Consumer Goods (Basel: ETAD, 1998).
6. I. Jäger, K. Schneider, P. Janak, D. Kralove, M. Huet, *Melliand Int. Textile* Reports English: 1-2/2005, E12-E14.
7. M.J. Prival, S.J. Bell, V.D. Mitchell, M.D. Peiperl, V.L. Vaughan, *Mutat. Res*., 1984, **136**, 33.
8. M.H. Zonoozi, M.R.A. Moghaddam, M. Arami, *Environ. Eng. Manag. J*., 2008, **7**, 695.
9. S. Sadri Moghaddam, M.R. Alavi Moghaddam, M. Arami, *J. Hazard. Mater*. 2010, **175**, 651.
10. R.V. Solomon, I. S. Lydia, J. P. Merlin, P. Venuvanalingam, *J. Iran. Chem. Soc*. 2012, **9**, 101.
11. C.P. Musteret, and C. Teodosiu, *Environ. Eng. Manage. J*., 2007, **6**, 175.
12. K.S. Tapan, and C. Nikhil, *Clean – Soil Air Water*, 2011, **39**, 984.
13. Q. Baocheng, Z. Jiti, X. Xuemin, Z. Chunli, Z. Hongxia, Z. Xiaobai, *J. Environ. Sci*., 2008, **20**, 704.
14. N.K. Amin, Desalination, 2008, **223**, 152.
15. A. Dalvand, M. Gholami, A. Joneidi, N.M. Mahmoodi, *Clean – Soil Air Water*, 2011, **39**, 665.
16. K. Pazdzior, A. Klepacz-Smolka, S. Ledakowicz, J. Sojka-Ledakowicz, Z. Mrozinska, R. Zylla, *Chemosphere*, 2009, **75**, 250.
17. G. Muthuraman, and T.T. Teng, *J. Ind. Eng. Chem*. 2009, **15**, 841.
18. R. Malarvizhi, M.H. Wang, Y.S. Ho, *World Appl. Sci. J.,* 2010, **8**, 930.
19. L. Al-Khatib, F. Fraige, M. Al-Hwaiti, O. Al-Khashman, *Am. J. Environ. Sci*. 2012, **8**, 510.
20. X. Wu, K.N. Huib, K.S. Huia, S.K. Lee, W. Zhoud, R. Chene, D.H. Hwang, Y.R. Cho, Y.G. Son, *Chem. Eng. J*., 2012, **180**, 91.
21. S.K. Bajpai, C. Navin, M. Manika, *Int. J. Environ. Sci*., 2012, **2**, 1609.
22. S. Saxena, S. Garg, A.K. Jana, *J. Environ. Res. Dev*. 2012, **6**, 424.
23. A. Rais, and K. Rajeev, *Clean – Soil Air Water*, 2011, **39**, 74.
24. V. Singh, A.K. Sharma, R. Sangh, *J. Hazard. Mater*., 2009, **166**, 327.
25. A. Anwar, G. Rumana, M.F. Wan, *Clean – Soil Air Water*, 2010, **38**, 153.
26. K.C. Kang, S.S. Kim, J.W. Choi, S.H. Kwon, *J. Ind. Eng. Chem.*, 2008, **14**, 131

27. X. Wang, Y. Guo, L. Yang, M. Han, J. Zhao, X. Cheng, *J. Environ. Anal. Toxicol*., 2012, **2**, 154.
28. M. Prasad, H-Y. Xu, S. Saxena, *J. Hazard. Mater*., 2008, **154**, 221.
29. G.M. Simu, S.G. Hora, M.E. Grad, E.N. Sisu, *Rev. Roum. Chim*., 2005, **50**, 113.
30. S. Muntean, G. Simu, M. Grad, R. Moldovan, *Proc. Symphos. 140 years from establishment of Romanian Academy,* 2006, 185.
31. Y.P. Qiu, J.L. Chen, A.M. Li, Q.X. Zhang, M.S. Huang, *Chin. J. Polym. Sci*., 2005, **23**, 435.
32. V. Dulman, C. Simion, A. Bârsănescu, I. Bunia, V. Neagu, *J. App. Polym. Sci*., 2009, **113**, 615.
33. H. Chen, and J. Zhao, 2009, *Adsorption* **15**, 381.
34 S.A. Umoren, U.J. Etim, A.U. Israel, *J. Mater. Environ. Sci.*, 2013, **4**, *75-86*
35. C. Valderrama, J.L. Cortina, A. Farran, X. Gamisans, F.X. de las Heras, *React. Funct. Polym*. **68**, 2008, 718.
36. U. Riaz, S.M. Ashraf, *Chem. Eng. J.*, **174**, 2011, 546.
37. Q.Y. Yue, Q. Li, B. Y. Gao, Y. Wang, *Sep. Purif. Technol*., **54**, 2007, 279.
38. C.Y. Kuo, C.H. Wu, J.Y. Wu, *J. Colloid. Interf. Sci*., 2008, **327**, 308.
39. G. Bayramoglu, B. Altintas, M. Yakup Arica, *Chem. Eng. J.*, 2009, **152**, 339.
40. M. Al-Ghouti, M.A.M. Khraisheh, M.N.M. Ahmad, S. Allen, *J. Colloid. Interf. Sci*., 2005, **287**, 6.
41. H. Hiroyuki, S. Fukuda, A. Okamoto, T. Kataoka, *Chem. Eng. Sci*. 1994, **48**, 2267.
42. M. N. Idrisa, Z. A. Ahmada, M. A. Ahmad, *IJBAS-IJENS*, **11**, 2011, 38.
43. S.D. Pardeshi, J.P. Sonar, A.M. Zine, S.N. Thore, *J. Iran. Chem. Soc*., 2013, **10**, 1159.
44. Y. Qiu, and F. Ling, *Chemosphere*, 2006, **64**, 963.
45. P. Monash, and G. Pugazhenthi, *Adsorption*, 2009, **15**, 390.
46. J. Raffiea Baseri, P.N. Palanisamy, P. Sivakumar, *E-J Chem.,* 2012, **9**, 1122.
47. M. Tayyebeh, A. Abbas, M.K. Hediye, A. Mazaher *J. Iran. Chem. Soc*., 2013, **10**, 481.
48. G. Albergina, and S. Fisichella, "Chimica delle Sostanze Colorante", Corso di Laurea in Chimica Industriale, 2005, Universita di Bologna
49. K.V. Kumar, S. Sivanesan, *Dyes Pigments*, **72**, 2007, 124-129.
50. P. K. Tripathi, M. Liu, L.Gan, *RSC Adv*., 2014, DOI:10.1039/C4RA01570C
51. Ö. Yavuz, and A.H. Aydin, *Pol. J. Environ. Stud*., 2006, **15**, 155.
52. J. He, S. Hong, L. Zhang, F. Gan, Y. S. Ho, *Fresenius Environ. Bull*., **19**, 2010, 2651
53. A. Kicsi, D. Bilba, M. Macoveanu, *Environ. Eng. Manage. J*., 2007, **6**, 205.
54. S.N.M. Yusoff, A. Kamari, W.P. Putra, C.F. Ishak, A. Mohamed, N. Hashim, I. Isa Md, *J. Environ. Protection*, 2014, **5**, 289.

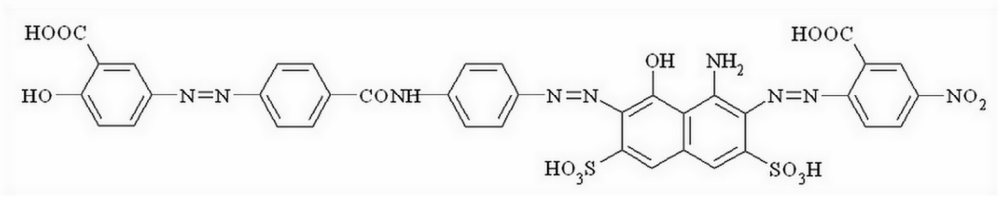

Fig. 1 Molecular structure of the AHDS dye
233x46mm (300 x 300 DPI)

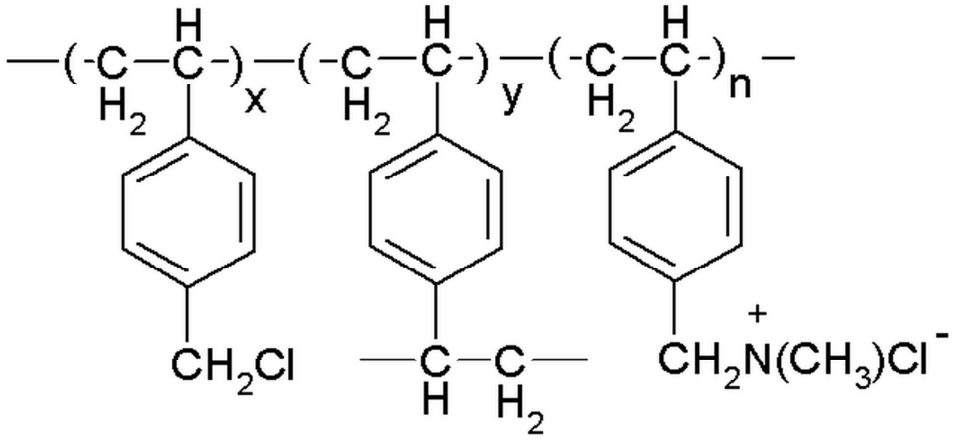

Fig. 2 Structural structure of the functionalized copolymer p(StDVB-NMe)
233x107mm (300 x 300 DPI)

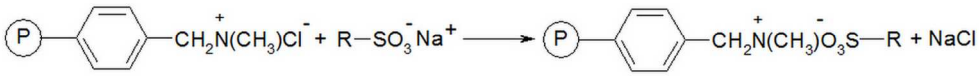

Fig. 3 Possible interaction process between AHDS dye and p(StDVB-ClMe)
233x26mm (300 x 300 DPI)

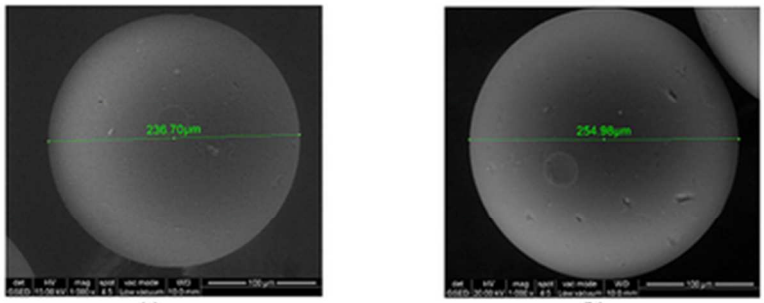

Fig. 4 SEM images for: (a) p(StDVB-NMe); (b) p(StDVB-NMe) with AHDS dye
34x14mm (300 x 300 DPI)

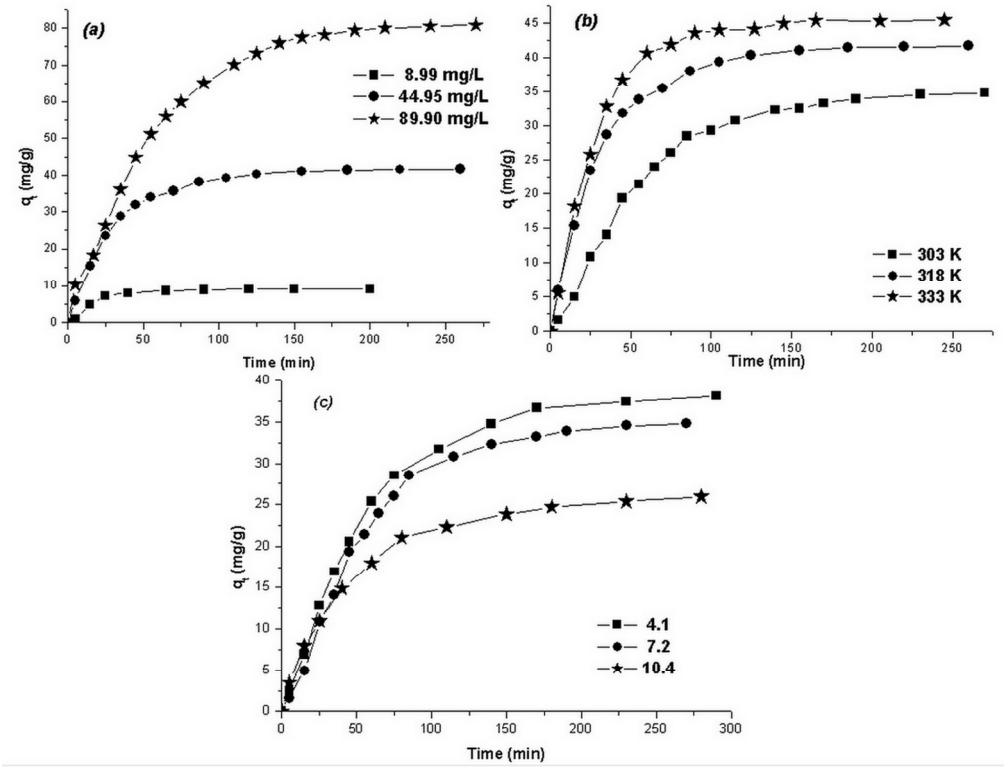

Fig. 5 Influence of the (a) initial concentration (1g L-1, 318 K, pH 6.8), (b) temperature (dye concentration 77.4 mg L-1, 1g L-1, pH 6.8), and (c) solution pH (dye concentration 77.4 mg L-1, 1g L-1, 318 K), on the AHDS dye removal
233x181mm (300 x 300 DPI)

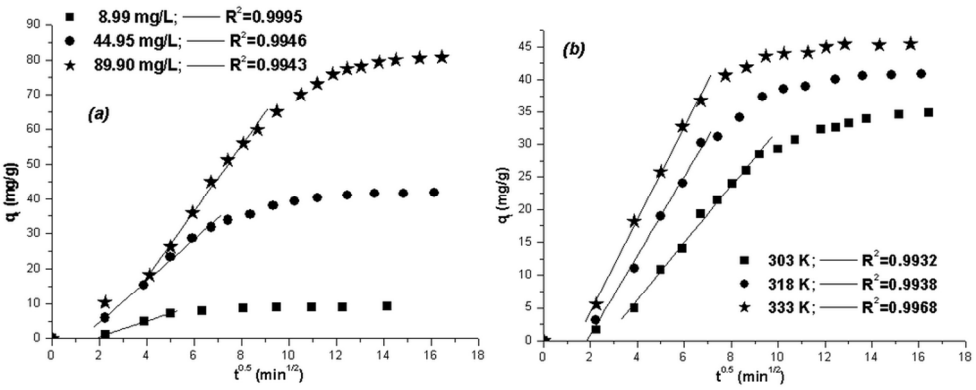

Fig. 6 The intraparticle diffusion of AHDS by p(StDVB-NMe); (a) initial concentration, (b) temperature.
233x89mm (300 x 300 DPI)

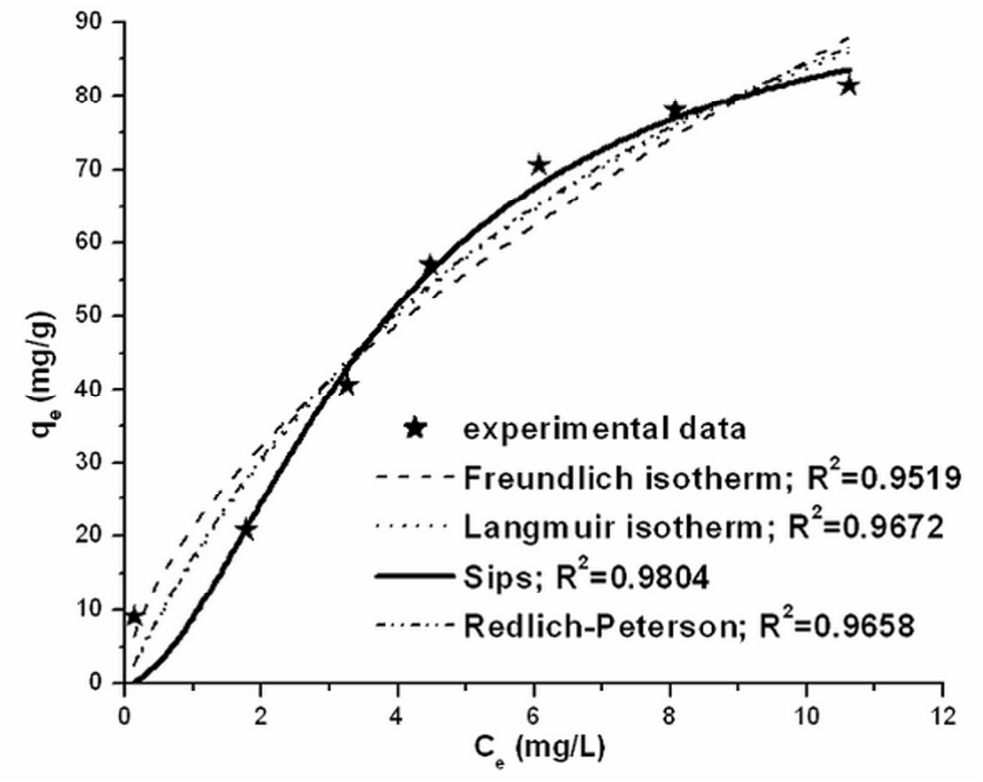

Fig. 7 Correlations between experimental data and different types of adsorption isotherms for AHDS dye adsorption on p(StDVB-NMe)
233x182mm (300 x 300 DPI)

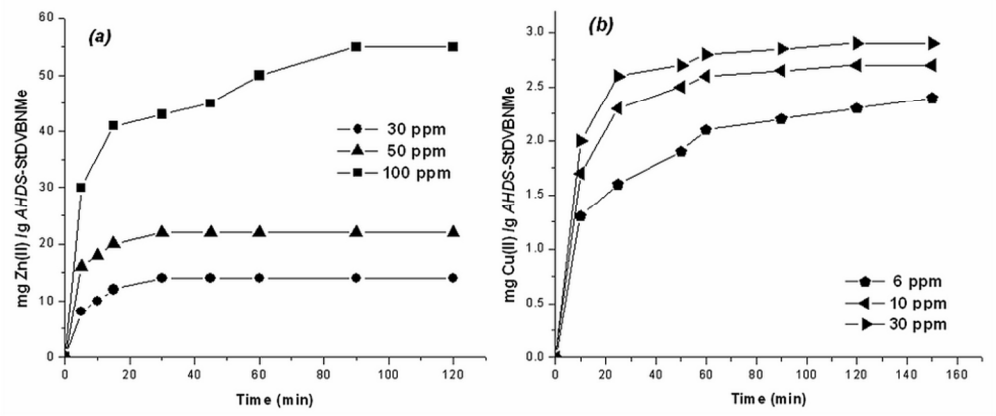

Fig. 8 Adsorption rates of heavy-metal ions: Cu(II) (a), Zn(II) (b), on AHDS-p(StDVBNMe) at 20oC
233x97mm (300 x 300 DPI)

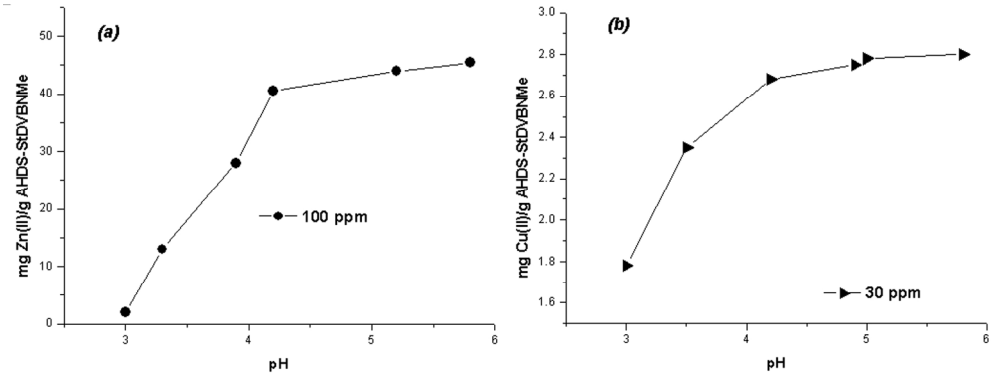

Fig. 9 Influence of the solution pH, on the heavy metal removal
233x86mm (300 x 300 DPI)

Table 1. The *AHDS* Dye Characteristics

AHDS dye formula	Synthesis	λ_{max} (nm)
$C_{37}H_{25}O_{15}N_9S_2$	salicylic acid←4,4'-diamino-benzanilide→H acid←*5*-nitroanthranilic acid	367; 551

Table 2. Elemental analysis of copolymer before and after dye adsorption.

Sample	*N %*	*O %*	*S %*	*Cl %*
p(StDVB-NMe)	4.93	4.71	-	11.95
p(StDVB-NM)-*AHDS*	7.09	15.08	0.70	6.71

Table 3. Influence of the process variables on the adsorption capacity of p(StDVB-NMe)

	Dye concentration (mg/L)			*Temperature (K)*			*pH*		
	8.99	*44.95*	*89.9*	*303*	*318*	*333*	*4.1*	*7.2*	*10.4*
q_e mg/g)	8.85	41.59	81.48	34.82	41.59	44.42	38.15	34.82	25.95
t_e (min)	40	110	170	170	110	105	190	230	235
η (%)	98.44	92.52	90.63	77.46	92.52	98.82	84.87	77.46	57.73

Table 4. Adsorption capacities of different adsorbent for the adsorption of dyes from aqueous solutions

Adsorbate	Adsorbent	Adsorption capacity q_t (mg/g)	Reference
Direct blue 3B	Poly(*N*-vinyl-2-pyrrolidone-*co*-acrylonitrile) treated with hydroxylamine–hydrochloride	7	[35]
Methylene Blue	poly (vinyl alcohol)	13.8	[34]
Acid Blue 29	Macroporous polystyrene cross-linked with divinylbenzene (Purolite A-520E)	48.2	[36]
Disperse Red S-R	EPI-DMA/bentonite	51,16	[37]
Direct Yellow 86 Direct Red 224	Carbon nanotubes	56.2 61.3	[38]
Crystal Violet	Grafted Poly(glycidylmethacrylate)	76.8	[39]
Methylene Blue	ZnAPSO 34	14.49	[51]
Methylene Blue	Rectorite	89.4	[52]
AHDS	p(StDVB-NMe)	97.42	[this study]

Table 5. First order and pseudo-second order adsorption rate constant, and comparison of experimental and calculated q_e values for adsorption of *AHDS* dye on p(StDVB-NMe)

C_0 (mg/L)	$q_{e,exp}$ (mg/g)	First order kinetic			Second order kinetic			Intraparticle diffusion		
		$q_{e,calc}$ (mg/g)	k_1 (min^{-1})	R^2	$q_{e,calc}$ (mg/g)	k_2 (mg/gmin)	R^2	k_i ($mg/gmin^{0.5}$)	l	R^2
8.99	8.85	6.30	$3.42 \cdot 10^{-2}$	0.9628	9.65	$1.01 \cdot 10^{-2}$	0.9986	2.232	-3.91	0.9995
44.95	41.59	36.91	$2.64 \cdot 10^{-2}$	0.9876	45.64	$8.94 \cdot 10^{-3}$	0.9963	5.967	-7.26	0.9946
89.9	81.48	99.94	$2.25 \cdot 10^{-2}$	0.9893	88.52	$2.08 \cdot 10^{-4}$	0.9966	9.449	-20.14	0.9943
Temp (K)										
303	34.82	39.74	$2.02 \cdot 10^{-2}$	0.9892	34.27	$3.83 \cdot 10^{-4}$	0.9989	4.369	-11.31	0.9932
318	41.59	46.84	$2.66 \cdot 10^{-2}$	0.9854	41.66	$7.23 \cdot 10^{-4}$	0.9978	6.046	-11.18	0.9938
333	44.42	40.67	$3.23 \cdot 10^{-2}$	0.9203	46.51	$9.81 \cdot 10^{-4}$	0.9948	7.066	-9.72	0.9968

Table 6. The adsorption isotherms models

Isotherm	Ecuation	
Freundlich	$q_e = K_F C_e^{1/n}$	(7)
Langmuir	$q_e = \frac{q_m K_L C_e}{1+K_L C_e}$	(8)
Sips	$q_e = \frac{q_m K_S C_e^{1/n}}{1+K_S C_e^{1/n}}$	(9)
Redlich-Peterson	$q_e = \frac{K_{RP} C_e}{1+\alpha_{RP} C_e^{\beta}}$	(10)

Table 7. Adsorption isotherm parameters for the *AHDS* dye adsorption on p(StDVB-NMe)

Models / Parameters	*Freundlich*	*Langmuir*	*Sips*	*Redlich-Peterson*
K_F (mg/g(mg/L)$^{-1/n}$)	21.31	-	-	-
n	1.67	-	0.58	-
q_m (mg/g)	-	151.04	97.42	-
K (L/mg)	-	0.12	0.27	-
K_{RP} (L/g)	-	-	-	19.77
α_{RP} (mg/L)$^{-\beta}$	-	-	-	0.15
β	-	-	-	0.95
R^2	0.9519	0.9672	**0.9804**	0.9658
χ^2	46.73	31.89	**23.83**	41.54

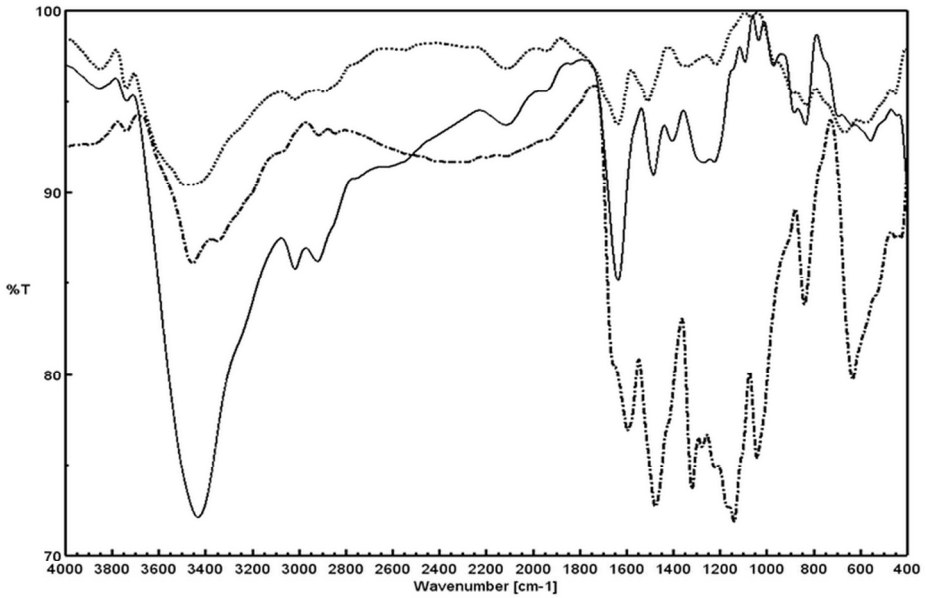

Supp. Figure 1. FT-IR spectra of (·····) p(StDVB-NMe); (—) AHDS; and (-·-·-·-) AHDS-p(StDVB-NMe)

SuppFig 1. FT-IR spectra
233x152mm (300 x 300 DPI)

Supp. Fig. 1a. FT-IR spectra of p(StDVB-NMe)

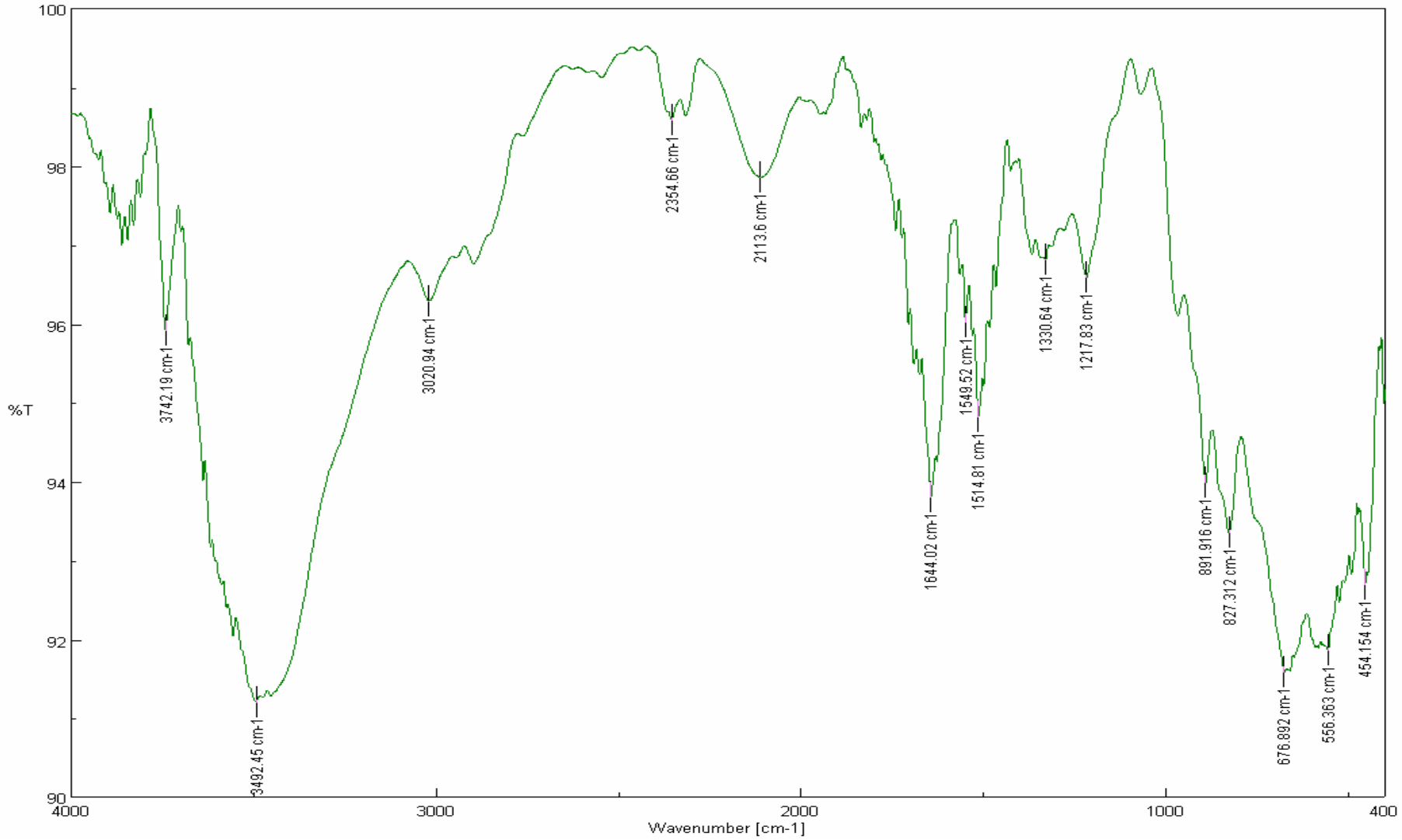

Supp. Fig. 1b. FT-IR spectra of *AHDS* dye

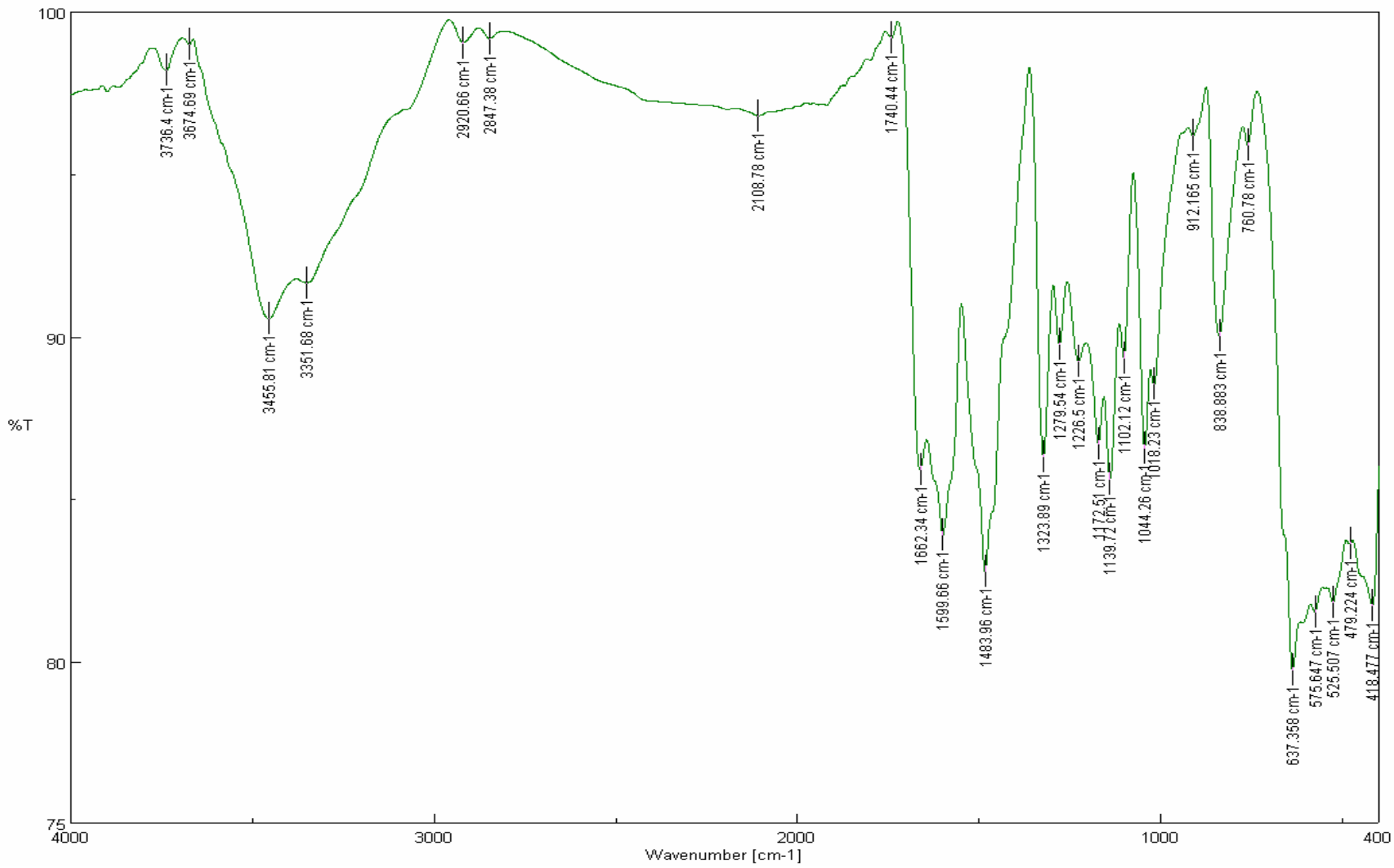

Supp. Fig. 1c. FT-IR spectra of *AHDS*-p(StDVB-NMe)